energies

MDPI

Article

Application of Solid-State Transformers in a Novel Architecture of Hybrid AC/DC House Power Systems

Fabio Bignucolo and Manuele Bertoluzzo *

Department of Industrial Engineering, University of Padova, via Gradenigo 6/a, 35131 Padova, Italy; fabio.bignucolo@unipd.it

* Correspondence: manuele.bertoluzzo@unipd.it; Tel.: +39-049-827-7923

Received: 9 June 2020; Accepted: 30 June 2020; Published: 3 July 2020

Abstract: The ongoing diffusion of solid-state DC/DC converters makes possible a partial migration of electric power systems from the present AC paradigm to a future DC scenario. In addition, the power demand in the domestic environment is expected to grow considerably, for example, due to the progressive diffusion of electric vehicles, induction cooking and heat pumps. To face this evolution, the paper introduces a novel electric topology for a hybrid AC/DC smart house, based on the solid-state transformer technology. The electric scheme, voltage levels and converters types are thoroughly discussed to better integrate the spread of electric appliances, which are frequently based on internal DC buses, within the present AC distribution networks. Voltage levels are determined to guarantee high safety zones with negligible electric risk in the most exposed areas of the house. At the same time, the developed control schemes assure high power quality (voltage stability in the case of both load variations and network perturbations), manage power flows and local resources according to ancillary services requirements and increase the domestic network overall efficiency. Dynamic simulations are performed, making use of DIgSILENT PowerFactory software, to demonstrate the feasibility of the proposed distribution scheme for next-generation smart houses under different operating conditions.

Keywords: hybrid AC/DC house; ancillary services; battery energy storage system; solid state transformer; smart house

1. Introduction

In the last century, AC power systems became common practice thanks to the transformer, enabling the change of voltage levels and reaching higher efficiency over long distance power transmission, which were the main drawbacks of DC power systems. Furthermore, the exploitation of the rotating magnetic field has made possible a simple, robust and not expensive bi-directional conversion between mechanical and electric energy.

Nowadays, the ever-growing diffusion of power electronic-based load, along with the integration of static generators exploiting renewable energy sources (RESs), are paving the way for a partial comeback of DC systems. The idea of converting present AC power systems into DC ones emerged some decades ago [1], following the emergence of the smart grid concept [2]. Recent studies on this topic aim at investigating the DC supply in distribution networks in terms of system design and architecture, voltage levels, protection and integration of AC common devices. An overview on DC distribution systems is presented in [3], where achievable advantages, such as stability and efficiency, are counterpoised to the lack of standards (e.g., technical laws and grid codes) and effective protection schemes. Different AC/DC conversion strategies are addressed in terms of voltage levels, technologies and topology, depending on the future evolution of electric devices, in [4].

The growing international sensibility to the containment of CO_2 emissions encourages the increasing exploitation of the electricity vector, which allows the reaching of a higher efficiency of appliances, in comparison to fossil fuel-based ones. In this process, full-electric houses are progressively emerging, particularly thanks to high levels of integration between electric components and the economic advantages obtainable by self-supplying the loads through local RESs (e.g., photovoltaic plants). In addition, static converters are more and more widely used to interconnect storage systems, chargers of electric vehicles and residential advanced appliances (induction cooking, home entertainment devices, computers, etc.), which make use of an internal DC bus.

The recent interest in residential DC microgrids, where distributed generation, controllable loads and storage systems are managed through control architectures to locally share the produced energy, requires further investigations [5,6]. It has been demonstrated that significant advantages, such as high power quality and loss reduction, are easily achievable with the DC approach [6,7], even if safety issues require a galvanic insulation between sensible loads and the main grid.

In this context, the solid-state transformer (SST) could play an interesting role. The aim of the SST is to provide variable step-up or step-down voltage transformation and an automatic voltage regulation through a solid-state apparatus and a high frequency transformer. The concept of the SST is encountered for the first time in the patent of Mcmurray [8], even if the name SST was introduced subsequently by Brooks et al. in [9]. Nevertheless, the limitations of the static switch technologies precluded the development of such an invention for several years, which faced problems concerning its weight, volume and efficiency. After the spread of semiconductor devices, the SST began to be considered as a possible solution to replace the conventional transformer in applications such as traction and smart grids [10]. The different architectures of SSTs can be basically divided into: (i) single-stage (AC/AC); (ii) two-stage (AC/DC-DC/AC); and (iii) three-stage SST (AC/DC-DC/DC-DC/AC) [11]. Despite the higher cost, the three-stage configuration offers more controllability and two DC links available, usually one in the high voltage (HV) and one in the low voltage (LV) side.

In traction applications, where volume and weight represent an issue, the bulky low-frequency transformer plus the back-to-back converter are replaced by a smaller and lighter SST, thus improving the overall efficiency of the traction system and providing more space for passengers [12]. On the other hand, when referring to smart grid applications, the controllability and availability of the DC link is the most desirable feature. Indeed, the SST can facilitate the integration of renewable energy sources and storage systems either in DC or AC buses [13,14].

In recent years, a novel concept of SST has been developed, the so-called smart transformer [15]: an SST which connects the medium voltage (MV) grid to the LV grid, replacing the conventional distribution transformer. In smart grid applications, the size of the SST has a limited impact, whilst its advantages stand in the services it can provide to both MV and LV grids, such as reactive power compensation, islanding capabilities and power quality.

Considering the possible future developments in the residential field, this paper describes the conceptual design of a combined AC/DC multi-level smart house architecture, with the novelty of exploiting the SST technology in the domestic network domain. A rational proposal is presented by the authors, with the definition of possible layout, components, voltage levels and base control schemes. Dynamic simulations of the domestic network are performed using conventional and well-grounded models of its main components (power converters, PV plants) to demonstrate the main advantages of the proposal with respect to existing connection schemes in terms of increased voltage stability and power quality. This scheme is also able to optimally integrate load, generation and storage management, aiming to provide ancillary services to the distribution network, such as voltage regulation and congestion reduction [16], dynamic mitigation of voltage sags and harmonic distortion [17], power factor correction, network stability support in terms of active and reactive power modulation (according to grid codes [18,19]) and phase currents balancing to compensate voltage unbalance issues [20–23].

In the following, Section 2 introduces the proposed architecture in comparison with the current AC paradigm, Section 3 discusses each part of the described hybrid solution, whereas the developed control strategies applied to the electronic power converter are described in Section 4. Section 5 briefly introduces the numerical case study and illustrates the main results in terms of dynamic simulations. Finally, main conclusions are drawn in Section 6.

2. AC/DC Household System Conceptual Proposal

Domestic electric systems are expected to significantly evolve in the near future, due to the recent technological advancements and the introduction of the smart house concept [24]. New devices, such as electric cooling and heating (air conditioners and heat pumps), induction cooking, electric vehicles, photovoltaic panels (PVs), energy storage systems (ESSs) and other modern appliances are expected to progressively diffuse in the existing electric system.

Without the management of loads and local resources, this appliance evolution requires end-users to increase their connections' rated power, contractually agreed with the distribution system operator (DSO). Consequently, the maximum power exchange with the network could rise from the present values (e.g., 3–6 kW in the Italian residential context) up to 15–20 kW or more (considering the electric vehicle fast charge requirements). In this case, the present best practice is to impose a three-phase connection between the end-user and the LV network (phase-to-phase rated voltage V_{AC} = 400 V, neutral wire usually available), as depicted in Figure 1a. In comparison with the single-phase connection to the grid, this configuration allows the reduction of line currents and power losses due to a more balanced power absorption. Maintaining the currently applied house network architecture, as represented in the figure, single-phase loads (rated voltage 230 V) are distributed on the three phases, whereas three-phase appliances and local sources, such as high-power loads and generators (photovoltaic generator and storage unit inverters), are connected to a dedicated bus (rated voltage 400 V).

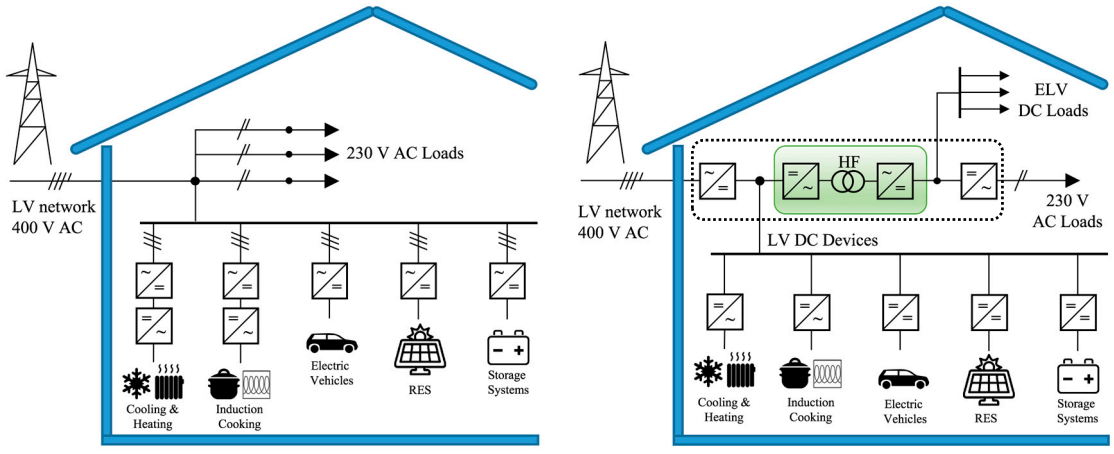

Figure 1. Electric schemes for a residential building hosting a huge penetration of electric devices: (**a**) Traditional network architecture based on AC internal distribution; (**b**) Conceptual representation of the innovative AC/DC topology, with three available voltage levels (according to appliance rated power and safety requirements) and partial galvanic insulation (realized through the DC/DC module of the solid state transformer (SST)).

Unfortunately, this approach does not consider that the majority of household appliances operate internally on DC voltage, such as TVs, computers, LED and future organic-LED lighting (OLED), PV generators, ESSs, etc. Some other devices (e.g., induction cooking systems and appliances with variable speed drive motors, such as modern refrigerators, heat pumps, washing machines, etc.) are required to work at a regulated frequency to maximize their efficiency, which necessarily involves

conversion from the main grid industrial frequency, usually through an intermediate DC stage. An overall efficiency improvement could be achieved by reducing the number of conversion stages and considering the higher efficiency of the DC/DC converters, in comparison to AC/DC converters [7,25].

The SST seems to be one of the most promising technologies to integrate the abovementioned elements in a house domain with internal DC buses, considering that AC appliances are still diffused (even if they are supposed to be slowly replaced by DC appliances) [4,26–28]. In the application presented here, conceptually depicted in Figure 1b, the SST (represented by the shape with a dashed edge in the figure), is the core of the proposed household hybrid system and consists of three modules in series: an AC/DC converter (the interface with the distribution network), a high frequency (HF) DC/DC converter, highlighted by the green shape and an inverter. In this way, several buses with different characteristics (AC or DC, voltage level) are available to supply loads with specific requirements. The benefits and limits of this scheme, in comparison with the current AC standard, are discussed in detail in the following sections with the support of dynamic simulations.

3. Detailed Internal Scheme of the Hybrid AC/DC House

Whereas the conceptual architecture of the hybrid AC/DC smart house, based on SST, is introduced above (Figure 1b), this section reports the results of a preliminary design in terms of technical information, detailed system topology, a converter sizing procedure and control strategies. The system has been modeled with the simulation software PowerFactory (version 2017, DIgSILENT GmbH, Gomaringen, Germany) (Figure 2), in particular, controllers have been developed by the authors making use of its native programming language. The proposed architecture (represented in the shape with dashed edge) is composed by:

- A three-phase connection to the LV network, realized through a bidirectional AC/DC converter which becomes the network interface between the domestic end-users and the DSO. The converter is equipped with a communication channel to exchange information with the environment (e.g., market data, control input from the DSO, tripping signals of network protections that interact with locally installed passive anti-islanding protections [29–31], etc.).
- An LV DC link of 700 V rated voltage (defined as LV according to [32]) connecting high power devices (electric vehicles, local generator, storage, washing machine, etc.) equipped with suitable plugs to ensure the safety standards.
- A *HF DC/DC* converter (included in the green shape in Figure 2) consisting of a voltage-controlled HF inverter, a HF transformer providing the galvanic insulation and two passive rectifiers that independently supply the two output ports.
- An extra low voltage DC bus of 50 V rated voltage (defined as ELV, according to [32]), for low power appliances (e.g., LED lighting, home entertainment devices, portable devices based on rechargeable batteries, etc.) and environments requiring high safety standards (such as bathrooms).
- An LV 230 V AC link to temporarily guarantee the transition from the present configuration to the future smart architecture. Present 230 V AC domestic loads could be supplied directly upstream from the main AC/DC converter with a higher efficiency, but in this case the galvanic insulation is not provided. Moreover, in a final DC house scenario, this link will not be implemented.

Due to the fast regulating action of static power converters, the SST allows both AC and DC stages to have different rated voltage levels and assures a very high voltage stability to all the supplied systems, since they are no longer affected by network voltage variations (both slow perturbations and transient phenomena). In addition, other achievable benefits are:

- The numerical reduction of AC/DC converters, replaced by more efficient DC/DC ones;
- Loss containment on cables connecting high power appliances and local sources, due to the higher voltage value in the LV DC link in comparison to the AC network voltage at the point of delivery (PoD);

- A reduced number of wires supplying high power loads: two (DC supply) instead of three (AC, four including the neutral wire);
- An ELV bus assuring high safety standards for supplying low power loads and for specific rooms with high safety requirements (e.g., bathroom, nursery, etc.);
- Controllability of active and reactive power exchanges between the end-user and the main network at the PoD, following DSO requirements, thus reducing the customer bill or enabling participation in the energy market;
- The optimized provision of ancillary services to the network by optimally controlling the main AC/DC converter and local sources [17], in accordance with grid code requirements or in case of economic reward;
- The equivalent increase in the distribution network hosting capacity, since the end-user's appliances are decoupled from the main grid and also correctly operate in the case of significant network voltage deviations at the PoD, e.g., caused by increased power flows in the distribution network;
- The absence of reactive power flows within the house network;
- The possible islanded operation of the residential network, intentionally disconnected from the main grid (e.g., public network outage in case of faults or scheduled maintenance activities).

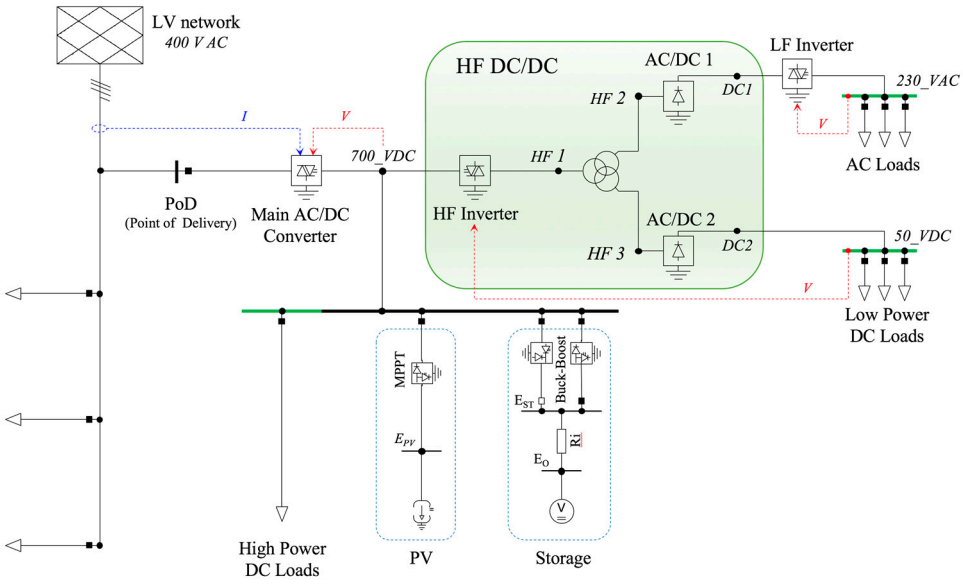

Figure 2. Detailed topology of the AC/DC hybrid configuration resulting from a preliminary design procedure, including the electric scheme, voltage levels and converter types.

In comparison with the current residential systems, the LV DC bus allows an efficient power exchange between the network, generation, storage and main loads, whereas an extra safety level is available for ELV appliances. The galvanic insulation realized through the HF transformer (i.e., with limited size and weight) reduces the electric risks, whereas short circuit currents are limited by electronic converters.

3.1. Main AC/DC Converter and LV DC Bus

The interface system between the LV network and the end-user consists of a pulse-width modulation (PWM) active rectifier (main AC/DC converter), which is sized depending on the main characteristics of the devices connected to the downstream DC link, i.e., load rated power, estimated coincidence factors, PV generator rated power, PV estimated production and ESS rated power. The main converter preliminary design procedure has to consider both the existing and the expected high-power appliances, considering that the fast charging of electric vehicles requires up to a few tens of kWs.

A more accurate design procedure of the main AC/DC converter could focus on limiting the inverter size by optimally managing the local sources. This allows the reduction of the device cost, the use of the converter at higher loading rates (i.e., with higher efficiency) and the containment of the connection rated power (i.e., reducing the electric bill). In this scenario, possible outages of either the generator or the ESS should be considered, thus a possible solution is classifying appliances as primary loads (in any way suppliable by the distribution network through the main AC/DC converter) and secondary loads (disconnected in case of anomalous operating conditions).

The main function of the AC/DC converter is to allow the bidirectional exchange of power between network and end-user, and to maintain the DC bus voltage level with a dedicated control (dotted red line in Figure 2). In addition, ancillary services are easily suppliable, such as:

- Active power regulation (*P/f*) to sustain network frequency (e.g., as proposed by the European standard [18] and required by the Italian grid code [19]);
- Reactive power modulation (*Q/V*), as required in [19];
- Reactive power management (according to power factor requirements or other logics [30]);
- LV network voltage balancing by responding to a DSO request (i.e., negative and zero sequence current injections), keeping constant the exchanged active power (absorbed or injected) [22].

Presently, no technical rules (e.g., grid codes, technical standards) define standardized values for the internal buses' voltages of the proposed SST-based residential network. In this work, the DC bus voltage V_{DC} downstream of the main AC/DC converter is set to 700 V, considering that a lower DC bus voltage does not ensure bidirectional power flows, whereas higher voltages would imply stricter insulation requirements. Thus, the converter modulation index m, identified by (1), is equal to 0.934 in rated conditions, allowing the converter bidirectional operation and DC link voltage regulation (as required by the project specifications), also in the case of network voltage variations.

$$V_{DC} = \left.\frac{2\sqrt{2}}{m \cdot \sqrt{3}} V_{AC}\right|_{0 \le m \le 1}; \qquad if \begin{cases} m = 1 \\ V_{AC} = 400\ V \end{cases} \rightarrow V_{DC} \approx 653\ V. \tag{1}$$

The selected voltage level allows a significant loss reduction in comparison with the present three-phase supply (V_{AC} = 400 V). Considering a generic load with active power P and power factor $cos(\varphi)$, the AC load current I_{AC} and the DC load current I_{DC} are evaluated as in (2).

$$I_{AC} = \frac{P}{\sqrt{3} \cdot V_{AC} \cdot \cos(\phi)}; \qquad I_{DC} = \frac{P}{V_{DC}}. \tag{2}$$

Considering a resistance R of the wires between the AC/DC converter and loads, Equation (3) evaluates the ratio r between losses in a traditional AC scheme (L_{AC}) and losses in the proposed approach (L_{DC}). It is demonstrated how AC losses are 1.53 times the ones in the DC case (if the AC load operates at unity power factor), or higher (in the case $cos(\varphi) < 1$).

$$r = \frac{L_{AC}}{L_{DC}} = \frac{3 \cdot R \cdot {I_{AC}}^2}{2 \cdot R \cdot {I_{DC}}^2} = \frac{{V_{DC}}^2}{2 \cdot {V_{AC}}^2 \cdot \cos^2(\varphi)} = \frac{1.53}{\cos^2(\varphi)} \geq 1.53 \tag{3}$$

The selected rated voltage could require a dedicated wiring and innovative technologies for the secure load connection [33]. Aiming at reducing the wire insulation requirements, the two terminals are assumed to be managed at +/−350 V referred to the ground potential.

3.2. DC/DC Converter Including High Frequency Transformer

The advanced design of the proposed domestic network architecture identifies the use of a DC/DC converter with two output voltage levels (with reference to Figure 2, 325 V at bus *DC1* and 50 V at bus *DC2*) as the optimal solution. The first voltage level is introduced to supply a typical single-phase PWM inverter (*LF Inverter* in Figure 2) for 230 V AC loads, if required. The second level directly

supplies low power DC loads with high safety specifications, i.e., galvanic insulation and rated voltage lower than the voltage threshold for ELV systems, intrinsically guaranteeing the human safety against direct or indirect contacts (European standard [32]). In this project, the rated voltage of 50 V has been chosen as indirect protection against direct contacts (as justified by the Italian technical standards), according to other literature [34,35]. Only buses *700_VDC*, *50_VDC* and *230_VAC* (drawn in green in Figure 2) are available for the connection of end-user appliances, whereas all the other nodes are inaccessible internal stages of converters.

The DC/DC converter consists of an HF inverter, a three-windings transformer and two diode rectifiers. The component *HF Inverter* is a PWM inverter with a 400 V AC output voltage (node *HF1*) and sized for around 3 kVA or less, since present AC loads are assumed to gradually disappear in the future and the rated power of ELV DC loads is generally low. In this work, the HF circuit design frequency is set to 20 kHz to reduce the DC/DC converter size and weight. Aiming to simplify the overall *HF DC/DC* system by adopting diode rectifiers on the output buses, the *HF Inverter* is entrusted with the regulation of the voltage at the bus *50_VDC* (feedback signal represented by the dotted red arrow in Figure 2). The voltage regulation at the DC/DC converter output node *50_VDC* can be performed by adopting any of the various technologies currently under investigation, with a comparatively low switching frequency. A possible method considers a resonant circuit and regulates the voltage acting on the inverter frequency modulation or adjusting the amplitude of the voltage first harmonic using the phase shift technique [36]. In this case, the output voltage regulation is obtained by varying the delay among the power switch triggering signals. The resonant circuit significantly reduces harmonic distortion and losses, even at a switching frequency equal to the HF bus frequency.

The three-windings transformer is introduced to obtain two voltage levels downstream of the passive rectifiers, i.e., to optimize the conversion efficiency in supplying the 230 V AC output bus rather than connecting an inverter with boost capability to node *DC2*. In the developed model, the rated voltage of nodes *HF1* and *HF2* are 241 V and 37 V, respectively. Converters *AC/DC1* and *AC/DC2* are diode rectifiers, instead of controlled rectifiers, to reduce costs and avoid possible reactive power flows in the transformer.

4. Regulating Strategies and Control Models

One of the most significant benefits of the proposed hybrid AC/DC architecture is the high voltage stability of all the output buses, even in the case of both sudden load changes and huge network voltage perturbations. As depicted in Figure 2, each output node is stabilized by a dedicated fast-regulating electronic device, autonomously driven by means of real-time local feedbacks. As a consequence, this control strategy does not require any centralized control or communication structure. Furthermore, loads are considered as passive devices without any load sharing control method (as usually done in microgrids [37]). In the following, control schemes and implementation choices are described.

4.1. Main AC/DC Converter Control Strategy

A schematic representation summarizing the control strategy applied to the element *Main AC/DC Converter* is shown in Figure 3a. All the functions listed in Section 3.1 can be performed by the proposed scheme. Two measurement devices (DC Voltage and AC Voltage) are installed at nodes *700_VDC* and *400_VAC* to provide both the AC and the DC voltage values, whereas the phase-locked loop (block PLL) allows the inverter to correctly synchronize with the network voltage [38,39]. Additional inputs may be DSO signals specifying the ancillary services to be provided (signal service) and negative or zero sequence current set-points (I_2, I_0) for feeder current balancing. Alternatively, these signals could be directly evaluated by the end-user (under DSO request) from feeder measurements (dotted blue line in Figure 2). Current set-points, defined in the block *Control Scheme*, drive the element *Main AC/DC Converter*. Signals $I_{1,REF}$, $I_{2,REF}$ and $I_{0,REF}$ are the positive, the negative and the zero sequence reference currents to be injected into the LV network, respectively.

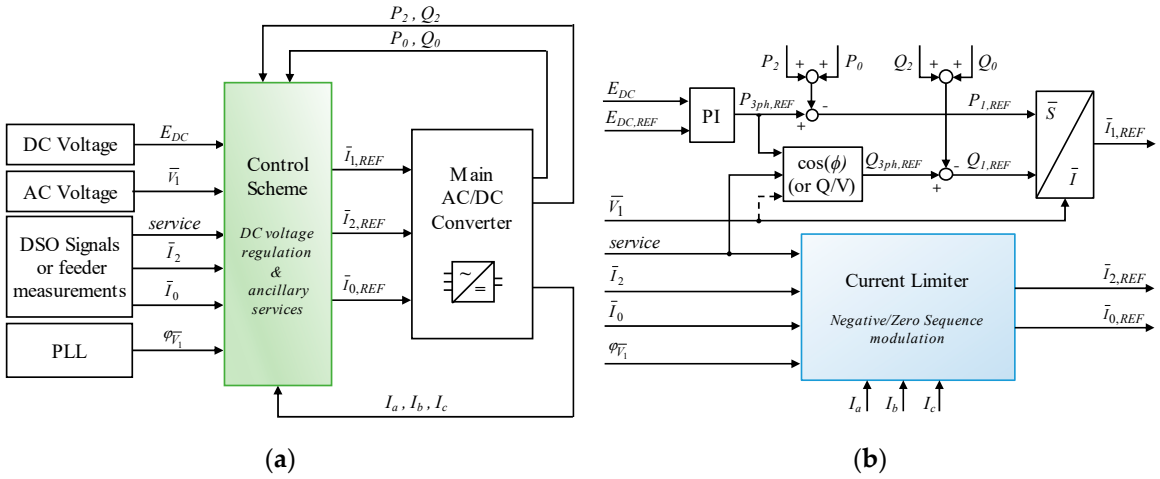

Figure 3. Control strategy for the bidirectional converter "*Main AC/DC Converter*", which acts as an interface between the distribution network and the end-user: (**a**) Complete control scheme regulating the converter to both maintain a stable DC voltage at node *700_VDC* and provide network ancillary services; (**b**) Inner structure of the block "*Control Scheme*" in (**a**), which evaluates the current reference signals.

Aiming to maintain the total three-phase active and reactive power, negative and zero sequence active/reactive power components (P_2/Q_2 and P_0/Q_0 in Figure 3a, respectively) are computed (on the basis of voltage and current measurements) at the converter terminals. The absolute phase current values (I_a, I_b, I_c) are used as feedback to avoid instantaneous violations of the converter capability threshold (AC side rated current) by limiting the negative and zero sequence current injections (i.e., reducing the network balancing regulation).

The block *Control Scheme* of Figure 3a is detailed in Figure 3b. Two independent branches evaluate the current reference signals, the upper one for the positive sequence current component, the other one for the negative and zero sequence current components. The total three-phase reference active power $P_{3ph,REF}$ is computed by a proportional–integral (PI) controller to regulate the bus voltage at node *700_VDC* (E_{DC}), whereas the total reactive power $Q_{3ph,REF}$ is derived according to DSO requirements, both the constant power factor and controlled reactive exchange (Q/V function, as required by [19]) are implemented operating modes.

Since the AC/DC converter is controlled to regulate the DC bus voltage V_{DC} and the reactive power exchange with the main network Q (V_{DC}-Q mode), the P/f regulation has to be directly implemented in the control logics of both the PV and the ESS, according to future prescriptions. In detail, although the active power modulation can be entirely required by the PV or to the ESS, sharing the contribution between the devices according to the ESS state of charge (SoC) and the PV actual generation seems the most effective solution. In general, modifying the power flows inside the residential system directly results in a small voltage variation at the bus *700_VDC*, which entails the action of the PI controller evaluating $P_{3ph,REF}$ in the *Main AC/DC Converter* controller.

From the evaluated power reference signals ($P_{3ph,REF}$ and $Q_{3ph,REF}$) and the measured negative and zero sequence active and reactive power components (P_2, Q_2, P_0, Q_0), the reference signals $P_{1,REF}$ and $Q_{1,REF}$ are obtained as in (4). Then, they are converted into current values by the operator S/I which implements (5). The signal $I_{1,REF}$ is expressed in the d-q coordinates system, whereas V_{1d} and V_{1q} are the voltage components on the direct and the quadrature axis, respectively. Since the d-q system is aligned to the positive sequence voltage in this case, $V_{1d} = V_1$ and $V_{1q} = 0$.

$$\begin{cases} P_{3ph} = \sum_{i=0}^{2} P_i = \sum_{i=0}^{2} \mathrm{re}(\overline{V}_i \cdot \bar{I}_i^*) \\ Q_{3ph} = \sum_{i=0}^{2} Q_i = \sum_{i=0}^{2} \mathrm{im}(\overline{V}_i \cdot \bar{I}_i^*) \end{cases} \quad (4)$$

$$\begin{cases} P_{1,REF} = I_{1d,REF} \cdot V_{1d} + I_{1q,REF} \cdot V_{1q} \\ Q_{1,REF} = I_{1d,REF} \cdot V_{1q} - I_{1q,REF} \cdot V_{1d} \end{cases} \quad (5)$$

Negative and zero sequence current references ($I_{2,REF}$ and $I_{0,REF}$) are provided by a dedicated controller (block Current Limiter) which dynamically reduces their amount if the converter capability threshold is close to be violated. The controller has been developed by one of the authors and is thoroughly discussed in [22].

4.2. HF DC/DC Converter and LF Inverter Control Strategies

The element *HF DC/DC Converter* consists of three passive devices (three-windings transformer and diode rectifiers) and the HF inverter, which controls voltage and frequency at the input terminals of the HF transformer (*V-f* mode). The voltage control aims at regulating the voltage stability at the bus *50_VDC* (node *DC2*), independently from the HF transformer working conditions (e.g., independently from the overall load connected at the bus *230_VAC*). This function is achieved by comparing the measured output voltage E_m with the reference value (E_{ref} = 50 V) to adjust the phase shift of the *HF Inverter* by means of a suitable PI controller. The switching frequency f_{ref} is set constant to 20 kHz, as depicted in Figure 4.

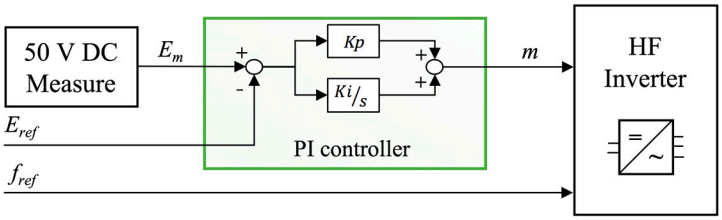

Figure 4. Control strategy for the converter "*HF Inverter*" regulating the *50_VDC* voltage bus.

The voltage at bus *DC1* is not directly regulated since it is not available for the connection of customer appliances, whereas the output AC voltage is stabilized by the downstream *LF Inverter*. This converter applies the same control logic depicted in Figure 4 (measuring the output voltage at the bus *230_VAC*) but, in this case, it adjusts the modulation index instead of the phase shift in order to generate a PWM output voltage with a modulating frequency of 50 Hz and a switching frequency of 20 kHz. Since the *HF DC/DC Converter* and the *LF Inverter* are series connected, the time constants of their controllers have to be appropriately designed. In this work, *LF Inverter* is assumed to regulate faster than *HF Inverter* to avoid unstable voltage transients. Similarly, the *Main AC/DC Converter* is the slowest of the whole system.

4.3. Photovoltaic System Model and Maximum Power Point Tracker Logic

The PV generator is modeled as an equivalent DC current source interfaced to the *700_VDC* bus through a DC/DC converter, as shown in Figure 5. The control scheme generates the current reference I_{PV} according to the actual irradiance, the estimated cell temperature and the PV module characteristics, such as rated power, open circuit voltage, short circuit current, *I-V* operating curve and temperature dependence. Since PV cells are represented as current sources, the overall generated power P_{PV} is obtained by modulating the PV array voltage E_{PV}. The regulation is applied, controlling the DC/DC converter voltage ratio $\alpha = E_1/E_{PV}$, where E_1 is the converter output voltage measured at node *700_VDC*. A dedicated internal algorithm reproduces the maximum power point tracking (MPPT) function.

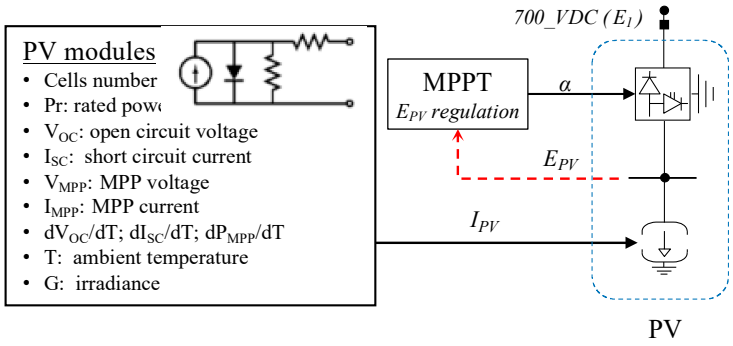

Figure 5. PV model developed in DIgSILENT PowerFactory to emulate the behavior of a PV generator depending on panel technical specifications and external conditions (weather, temperature, etc.).

4.4. Storage System Model

In general, the ESS is a device called on to exchange energy according to its SoC and to the external reference signal (*Reference Power*) provided by a dedicated logic, which implements different functionalities, such as (but not limited to):

- leveling the local power generation to mitigate RES fast perturbations (e.g., wind fluctuation, clouds) and to perform the daily peak shaving function;
- contributing to supplying the load peak power to reduce the contractually defined maximum power absorption (and consequently the end-user bill);
- minimizing the power exchanged by the end-user with the AC distribution network;
- providing the *P/f* regulation, or a part of it.

In this work, the third of the above listed modes is considered as the base logic for battery management. It should be noted that this property could be interpreted as an equivalent ancillary service provided to the network, since a significant increase in the network hosting capacity is directly obtained. Indeed, by suitably managing the storage system, the end-user is able to modulate the power exchange with the network, e.g., to minimize it, to maintain a fixed set-point or to respect specific thresholds in accordance with the DSO [40].

The model implemented in the simulation software (Figure 6) consists of the battery representation (an ideal voltage source with a variable resistor in series) and a buck–boost bidirectional converter. Both the source open circuit voltage E_{OC} and the battery equivalent resistance R_i are real-time evaluated according to the datasheet information and the battery SoC.

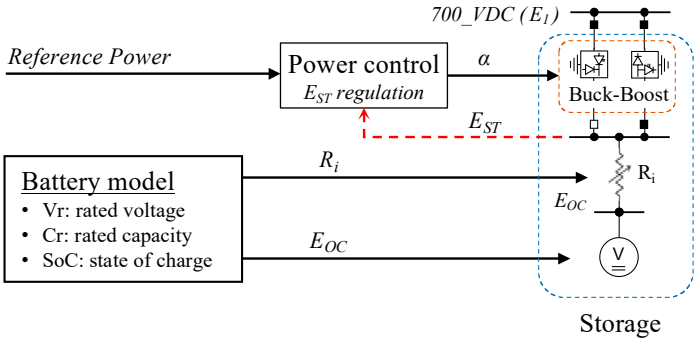

Figure 6. Battery model developed in DIgSILENT PowerFactory to emulate the behavior of the storage system as a function of the SoC and the required power exchange.

The power exchange is regulated by modulating the DC/DC converter voltage ratio $\alpha = E_1/E_{ST}$ through a PI controller depending on the input signal *Reference Power*, where E_{ST} is the voltage at the battery terminals.

5. Case Study and Results

The case study considers the residential system depicted in Figure 2. Considering the conceptual design stage of the proposed approach, root mean square (RMS) dynamic simulations are carried out to verify both the converter decoupling performances (in terms of voltage stability at the AC/DC house buses) and the power flow management in the end-user network. Conversely, current and voltage waveforms and their harmonic distortion (on both the AC and the DC buses), depending on the adopted converter technologies and investigable by means of electromagnetic transient (EMT) simulations, are not considered in this work.

Typical events, such as load perturbations, network voltage transients and ancillary service provision, are considered. The scope of the analysis is:

- demonstrating the voltage stability at all the three output buses (*700_VDC*, *50_VDC* and *230_VAC*) in the case of the fast variation of the load power absorption (Section 5.1);
- demonstrating the voltage stability of the same buses in case of the significant variation of the network voltage at the PoD (Section 5.2);
- verifying the effectiveness of the proposed control schemes in providing network ancillary services (Section 5.3), such as (i) Q/V regulation; (ii) network voltage balancing; and (iii) the regulation of the power exchange with the distribution network.

Transformer and converter technical specifications, in terms of rated voltages (V_r), rated power (S_r) and efficiency (η), are reported in Tables 1 and 2, respectively. Load absorption is variable over time, as described in the following.

Table 1. HF transformer technical specifications.

Winding 1—Node *HF1*	Winding 2—Node *HF2*	Winding 3—Node *HF3*
$S_{r,1}$ = 3 kVA $V_{r,1}$ = 400 V η = 98%	$S_{r,2}$ = 2 kVA $V_{r,2}$ = 241 V f = 20 kHz	$S_{r,3}$ = 1.2 kVA $V_{r,3}$ = 37 V

Table 2. Converter technical specifications.

Main AC/DC Converter	*HF Inverter*	*AC/DC1*	*AC/DC2*	*LF Inverter*
$V_{r,AC}$ = 400 V 3-ph $V_{r,DC}$ = 700 V S_r = 10 kVA η = 97%	$V_{r,DC}$ = 700 V $V_{r,AC}$ = 400 V 3-ph S_r = 3 kVA η = 98%	$V_{r,AC}$ = 241 V 3-ph $V_{r,DC}$ = 325 V S_r = 2 kVA η = 98%	$V_{r,AC}$ = 37 V 3-ph $V_{r,DC}$ = 50 V S_r = 1.2 kVA η = 98%	$V_{r,DC}$ = 325 V $V_{r,AC}$ = 230 V 1-ph S_r = 2 kVA η = 97%

5.1. Voltage Stability in the Case of Load Variations

With reference to Figure 2, three equivalent loads (represented with the constant impedance model) are connected at output nodes *700_VDC*, *50_VDC* and *230_VAC*. For each load, Table 3 reports the initial power absorption, the load variation and the time instant of the variation. Two scenarios are studied in detail: a) the instantaneous variation of the load absorption, to analyze the step response of the system in terms of output nodes' voltages and b) the ramp variation of the load absorption (time duration 0.05 s) to study a more realistic case. The initial PV generation is 4.3 kW, whereas the storage system is disconnected. The results of dynamic simulations are reported in Figure 7, showing the voltages of the node PoD, *700_VDC*, *50_VDC* and *230_VAC*, respectively. In scenario a), the 4 kW variation of *High Power DC Loads* causes the voltage to drop below 95% at bus *700_VDC*, but it is promptly restored by the action of the *Main AC/DC Converter* controller within the range V_r +/−0.5% in less than 0.07 s (Figure 7a). Similar voltage trends can be observed for the other two events. It is verified that the controllers of *HF Inverter* and *LF Inverter* are faster than the *Main AC/DC Converter*,

thus, unstable transients are avoided. In scenario b), voltage perturbations are considerably reduced thanks to the readiness of the control in realistic conditions (Figure 7b). Finally, Figure 7 shows that ordinary internal electric events are successfully faced without negatively affecting the output node voltage quality. Indeed, load variations cause fast voltage drops, but transients are perfectly restored in an extremely short time.

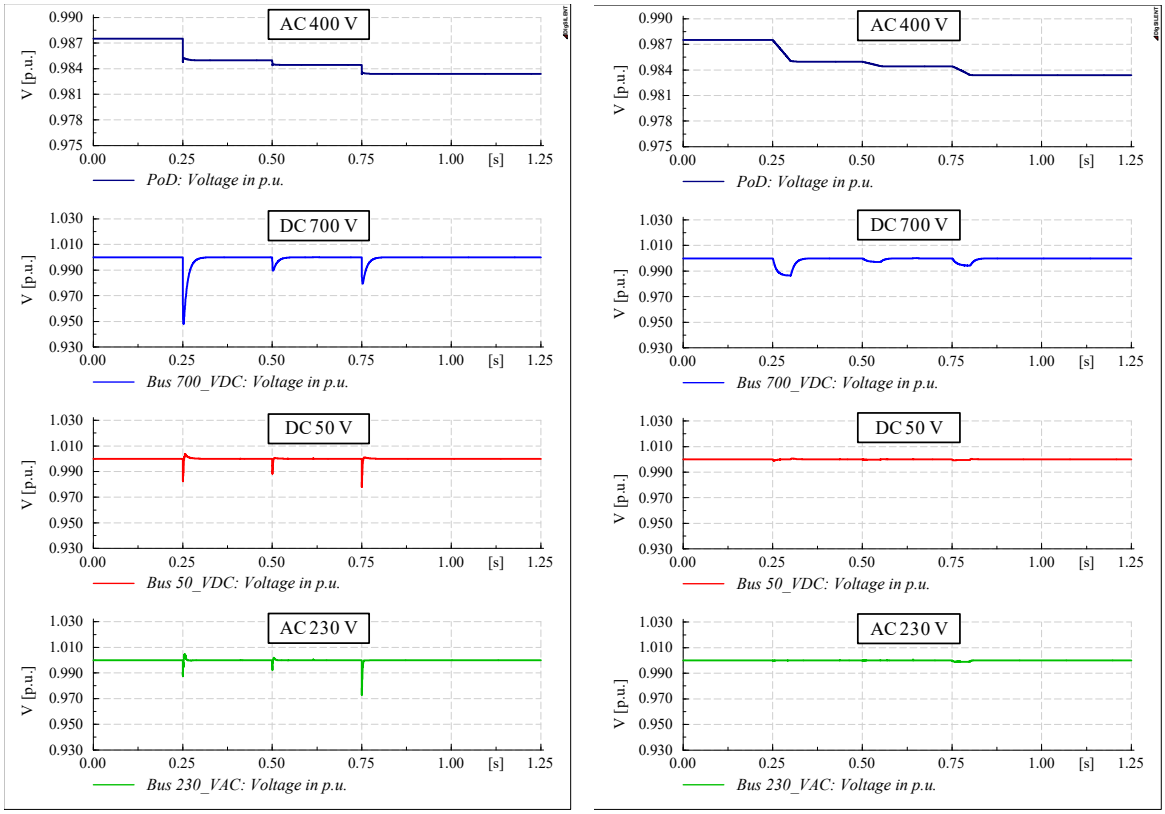

Figure 7. Voltage response to load variations, considering the point of delivery (PoD) and all the proposed architecture output nodes: (**a**) Step power variation; (**b**) Ramp power variation (ramp time 0.05 s).

Table 3. Load power and connection time.

	Output Node	Initial Load (kW)	Load Variation (kW)	Variation Time Instant (s)
High Power DC Loads	*700_VDC*	1.00	+4.0	0.25
Low Power DC Loads	*50_VDC*	0.05	+0.8	0.50
AC Loads	*230_VAC*	0.10	+1.5	0.75

5.2. Voltage Stability in the Case of LV Network Perturbations

This section investigates the performance of the *Main AC/DC Converter* in decoupling voltages of output buses from the grid voltage, thus maintaining the internal voltages at the rated values even in the case of fast network events. This feature could also be interpreted as an additional ancillary service towards the upstream LV network, since the DSO could regulate the network voltage in a wider range without impacting on the end-user operation and safety. In other words, from the DSO

viewpoint, this directly means a significant increase in the network hosting capacity (excluding line congestion management).

A representative simulation is reported in Figure 8, which shows the network voltage at node PoD, the reactive power exchange with the LV network and the voltage trends at output nodes (*700_VDC*, *50_VDC* and *230_VAC*). In particular, at t = 0.1 s, external events (e.g., a significant increase in other customers' absorption) cause a voltage drop of 10% at the node PoD, with a ramp of 0.01 s. This entails a voltage transient at output buses, in particular at the *700_VDC* node (bottom plot, red curve). However, the output node voltage perturbations (about 0.4%) are much lower than the one recorded in the distribution network (10%, at node PoD) and are rapidly compensated. The reactive power perturbation at t = 0.1 s is caused by the delay in the PLL measurement, which consequently leads to an imperfect converter synchronization with the network.

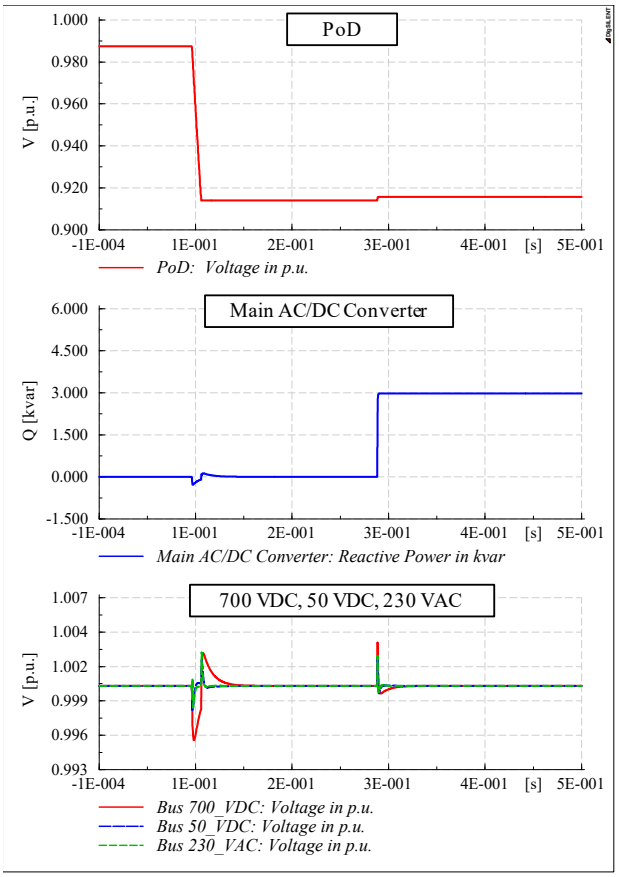

Figure 8. Voltage regulation at output buses during network voltage perturbations and *Q/V* stabilizing function provision.

5.3. Ancillary Services Provision

In this section, the proposed AC/DC architecture performances are tested in the case of ancillary service activation (*Q/V* function, network voltage balancing and active power exchange regulation). With reference to that previously reported Figure 8, the ability of the proposed controller in providing the *Q/V* function is verified. The stabilizing action is activated at t = 0.3 s, produces a reactive power exchange of about 3 kVAr and involves a small rise in the network voltage (the weak effects of the reactive power modulation in regulating voltage profiles in LV networks are discussed in [41]). At the same time, no significant voltage perturbations are observed at any of the house buses.

Figure 9 shows the benefits of the network voltage balancing ancillary service, activated at t = 0.2 s as a response to a DSO request. The negative sequence voltage v_2 measured at the node PoD (upper

plot) is progressively reduced from almost 2.0% to about 1.4% by intentionally unbalancing the phase current injections of the *Main AC/DC Converter* (middle plot). The controller depicted in Figure 3b limits this contribution when one of the phase currents reaches the inverter rated value I_r (phase-A at t = 0.26 s in the middle plot).

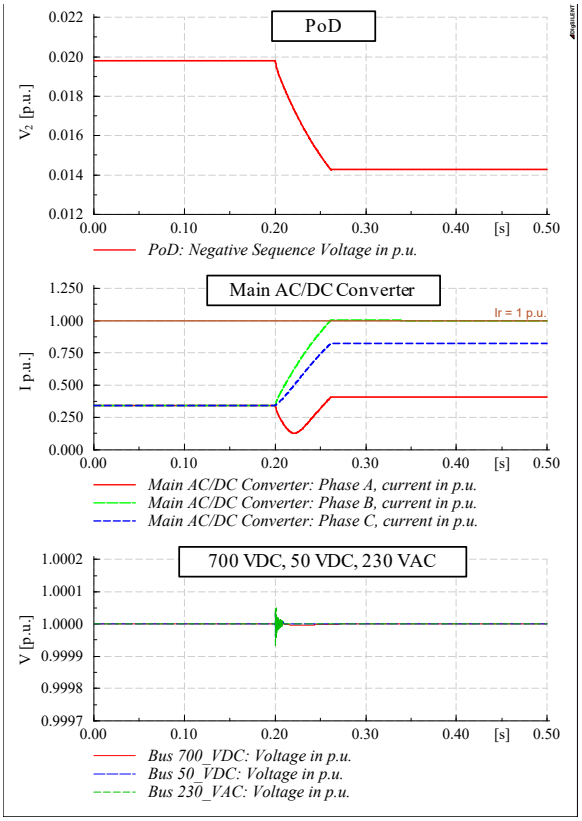

Figure 9. Negative sequence network voltage balancing ancillary service provided by the SST-based end-user.

Since the balancing service is still not specified by connection standards, its PI controller is set slower than other controllers to not affect the output bus voltage stability. This assumption is confirmed in the bottom plot of Figure 9, where the activation of the balancing function has negligible effects on house buses. Analogous results are obtainable, referring to the zero-sequence voltage (if the *Main AC/DC Converter* is equipped with the neutral connection).

The last simulation, reported in Figure 10, demonstrates the capability of the developed smart house system in controlling the power exchange with the main grid, keeping the output bus voltages regulated. In the model, this function is assigned to the ESS, therefore the signal *Reference Power* of Figure 6 is evaluated to minimize the power exchange with the grid according to the SoC range limits, and also in the case of variations in both the PV generation and the load consumption.

Two perturbations are considered: firstly, the local generation decrease of 3 kW at t = 1 s (e.g., reproducing a cloud darkening the PV panels) with a slow transient of 1 s (dotted blue line); later, a 3-kW load variation is experienced at t = 4 s with a ramp of 0.1 s. During both the events, the ESS correctly satisfies the request of controlling the power exchange with the network.

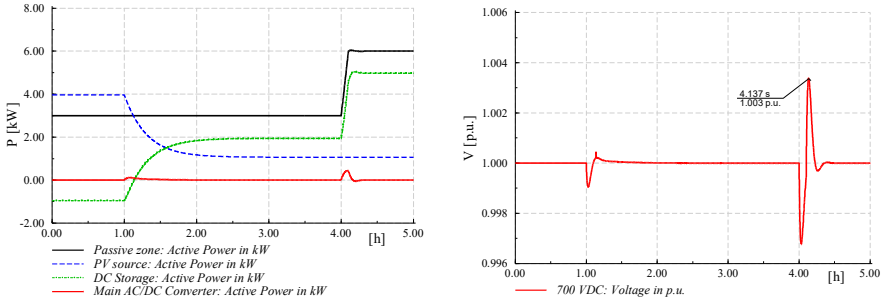

(**a**) (**b**)

Figure 10. Storage management aiming to reduce power exchange with the network: (**a**) Power flows; (**b**) Voltage of bus *700_VDC*.

The zero exchanged power set-point is restored in a few tens of milliseconds according to measurement delays (red line in Figure 10a). At the same time, the house bus voltages are constantly regulated by the *Main AC/DC Converter* (Figure 10b reports the voltage trend at bus *700_VDC*).

6. Conclusions

Power systems are nowadays experiencing both an increasing diffusion of solid-state power converters and a significant spread of modern electric devices and RES generators, which commonly have an internal DC stage. DC electric systems are currently under study in different fields (both transmission and distribution) and, particularly at the residential level, a progressive migration from the present AC-supplied houses to a novel concept of AC/DC smart houses is expected in the near future, even if standards are not defined yet.

This paper proposes and describes in detail a possible evolution of household AC electrical schemes towards a hybrid AC/DC architecture, able to accommodate the growing power flows consequent to the expected wider diffusion of electricity with respect to other energy vectors. The internal electric topology, voltage levels, converter types, control schemes and a sizing procedure are introduced and discussed. With the proposed approach, users have the chance to connect appliances to three buses with different voltage characteristics (DC 700 V, galvanic insulated DC 50 V and galvanic insulated AC 230 V). In particular: (i) the DC 700 V bus allows the connection of high power devices (heating, cooling, electric vehicle chargers, electric cooking devices, local generators and storage systems) with minimized losses; (ii) the galvanic insulated DC portion with a rated voltage of 50 V assures high safety levels for low power loads and specific rooms (bathroom, nursery, children's room); and (iii) the single-phase AC output bus (for traditional AC appliances) facilitates the progressive evolution of loads from present standards to a future DC supply.

Thanks to the static converter decoupling properties, the proposed SST-based architecture, regulated through the proposed control schemes, has the ability to provide both higher voltage stability at the house buses and ancillary services to the network (according to DSO requirements and potential economic remunerations), as demonstrated through dynamic simulations.

Author Contributions: F.B. and M.B. conceived the project and defined the smart house topology. F.B. realized the dynamic models in DIgSILENT PowerFactory, making use of the software programming language, whereas M.B. contributed by projecting the control schemes. All authors have read and agreed to the published version of the manuscript.

Funding: This research was funded by University of Padova, project "PRAT 2015—Smart power hub for AC/DC distribution in high efficiency residential applications".

Conflicts of Interest: The authors declare no conflict of interest.

References

1. Wicks, F. Evaluating alternatives for integrating distributed DC generation with AC power systems. In Proceedings of the IECEC 35th Intersociety Energy Conversion Engineering Conference and Exhibit, Las Vegas, NV, USA, 24–28 July 2000; Volume 2, pp. 763–766. [CrossRef]
2. Colak, I.; Kabalci, E.; Fulli, G.; Lazarou, S. A survey on the contributions of power electronics to smart grid systems. *Renew. Sustain. Energy Rev.* **2015**, *47*, 562–579. [CrossRef]
3. Hamad, A.A.; El-Saadany, E.F. Multi-agent supervisory control for optimal economic dispatch in DC microgrids. *Sustain. Cities Soc.* **2016**, *27*, 129–136. [CrossRef]
4. Patrao, I.; Figueres, E.; Sanfeliú, G.G.; González-Medina, R. Microgrid architectures for low voltage distributed generation. *Renew. Sustain. Energy Rev.* **2015**, *43*, 415–424. [CrossRef]
5. Kim, T.; Yun, J.; Qiao, W. A multiagent system for residential DC microgrids. In Proceedings of the IEEE Power & Energy Society General Meeting, Denver, CO, USA, 26–30 July 2015; pp. 1–5. [CrossRef]
6. Kakigano, H.; Miura, Y.; Ise, T.; Momose, T.; Hayakawa, H. Fundamental characteristics of DC microgrid for residential houses with cogeneration system in each house. In Proceedings of the IEEE Power and Energy Society General Meeting-Conversion and Delivery of Electrical Energy in the 21st Century, Pittsburgh, PA, USA, 20–24 July 2008; pp. 1–8. [CrossRef]
7. Kakigano, H.; Nomura, M.; Ise, T. Loss evaluation of DC distribution for residential houses compared with AC system. In Proceedings of the IPEC International Power Electronics Conference, Sapporo, Japan, 21–24 June 2010; pp. 480–486. [CrossRef]
8. Mcmurray, W. Power Converter Circuits Having a High Frequency Link. U.S. Patent 3517300, 23 June 1970.
9. Brooks, J.L.; Staab, R.I.; Bowers, J.C.; Niehaus, H.A. Solid StateRegulated Power Transformer with Waveform Conditioning Capability. U.S. Patent 4347474, 31 August 1982.
10. Huber, J.E.; Kolar, J.W. Solid-State Transformers: On the Origins and Evolution of Key Concepts. *IEEE Ind. Electron. Mag.* **2016**, *10*, 19–28. [CrossRef]
11. Qin, H.; Kimball, J. Solid-State Transformer Architecture Using AC–AC Dual-Active-Bridge Converter. *IEEE Trans. Ind. Electron.* **2012**, *60*, 3720–3730. [CrossRef]
12. She, X.; Huang, A.Q.; Burgos, R. Review of Solid-State Transformer Technologies and Their Application in Power Distribution Systems. *IEEE J. Emerg. Sel. Top. Power Electron.* **2013**, *1*, 186–198. [CrossRef]
13. Yu, X.; She, X.; Zhou, X.; Huang, A.Q. Power Management for DC Microgrid Enabled by Solid-State Transformer. *IEEE Trans. Smart Grid* **2013**, *5*, 954–965. [CrossRef]
14. She, X.; Yu, X.; Wang, F.; Huang, A.Q. Design and demonstration of a 3.6kV120V/10KVA solid state transformer for smart grid application. *IEEE Trans. Power Electron.* **2014**, *29*, 3982–3996. [CrossRef]
15. Liserre, M.; Buticchi, G.; Andresen, M.; De Carne, G.; Costa, L.F.; Zou, Z.-X. The Smart Transformer: Impact on the Electric Grid and Technology Challenges. *IEEE Ind. Electron. Mag.* **2016**, *10*, 46–58. [CrossRef]
16. Bignucolo, F.; Caldon, R.; Carradore, L.; Sacco, A.; Turri, R. Role of storage systems and market based ancillary services in active distribution networks management. In Proceedings of the CIGRE 43rd International Conference on Large High Voltage Electric Systems, Paris, France, 22–27 August 2010; pp. 1–9.
17. Banaei, M.; Salary, E. Mitigation of voltage sag, swell and power factor correction using solid-state transformer based matrix converter in output stage. *Alex. Eng. J.* **2014**, *53*, 563–572. [CrossRef]
18. *CENELEC TS 50549-1: Requirements for Generating Plants to be Connected in Parallel with Distribution Networks - Part 1: Connection to a LV Distribution Network above 16 A*; European Committee for Standards: Brussels, Belgium, January 2015.
19. *CEI 0-21: Reference Technical Rules for the Connection of Active and Passive Users to the LV Electrical Utilities*; Italian Electrotechnical Committee: Milan, Italy, July 2016.
20. Caldon, R.; Coppo, M.; Turri, R. Voltage unbalance compensation in LV networks with inverter interfaced distributed energy resources. In Proceedings of the IEEE International Energy Conference and Exhibition (ENERGYCON), Florence, Italy, 9–12 September 2012; pp. 527–532. [CrossRef]
21. Caldon, R.; Coppo, M.; Turri, R. Coordinated voltage control in MV and LV distribution networks with inverter-interfaced users. In Proceedings of the IEEE PowerTech, Grenoble, France, 16–20 June 2013; pp. 1–5. [CrossRef]

22. Savio, A.; Bignucolo, F.; Caldon, R. Contribution of MV Static Distributed Generation to Voltage Unbalance Mitigation. In Proceedings of the AEIT International Annual Conference, Capri, Italy, 5–7 October 2016; pp. 1–6. [CrossRef]
23. Alepuz, S.; Gonzalez, F.; Martin-Arnedo, J.; Martinez, J.A. Solid state transformer with low-voltage ride-through and current unbalance management capabilities. In Proceedings of the IECON 39th Annual Conference of the IEEE Industrial Electronics Society, Vienna, Austria, 10–13 November 2013; pp. 1278–1283. [CrossRef]
24. Kimura, N.; Morizane, T.; Omori, H. Power management unit for dc feeder in house (dc smart house). In Proceedings of the ICRERA International Conference on Renewable Energy Research and Applications, Nagasaki, Japan, 11–14 November 2012; pp. 1–5. [CrossRef]
25. Paajanen, P.; Kaipia, T.; Partanen, J. DC supply of low-voltage electricity appliances in residential buildings. In Proceedings of the CIRED 20th International Conference and Exhibition on Electricity Distribution-Part 1, Prague, Czech Republic, 8–11 June 2009; pp. 1–4. [CrossRef]
26. Bignucolo, F.; Bertoluzzo, M.; Fontana, C. Applications of the solid state transformer concept in the electrical power system. In Proceedings of the AEIT International Annual Conference, Naples, Italy, 14–16 October 2015; pp. 1–6. [CrossRef]
27. Yan, J.; Zhu, X.; Lu, N. Smart hybrid house test systems in a solid-state transformer supplied microgrid. In Proceedings of the IEEE Power & Energy Society General Meeting, Denver, CO, USA, 26–30 July 2015; pp. 1–5. [CrossRef]
28. Fontana, C.; Buja, G.; Bertoluzzo, M.; Kumar, K.; Wang, Q. Power and control characteristics of an isolated three-port DC-DC converter under DCM operations. In Proceedings of the IECON 42nd Annual Conference of the IEEE Industrial Electronics Society, Florence, Italy, 23–26 October 2016; pp. 4211–4216. [CrossRef]
29. Bignucolo, F.; Caldon, R.; Frigo, M.; Morini, A.; Pitto, A.; Silvestro, F. Impact of distributed generation on network security: Effects on loss-of-main protection reliability. In Proceedings of the UPEC 43rd International Universities Power Engineering Conference, Padova, Italy, 1–4 September 2008; pp. 1–5. [CrossRef]
30. Bignucolo, F.; Cerretti, A.; Coppo, M.; Savio, A.; Turri, R. Impact of Distributed Generation Grid Code Requirements on Islanding Detection in LV Networks. *Energies* **2017**, *10*, 156. [CrossRef]
31. Bignucolo, F.; Cerretti, A.; Coppo, M.; Savio, A.; Turri, R. Effects of Energy Storage Systems Grid Code Requirements on Interface Protection Performances in Low Voltage Networks. *Energies* **2017**, *10*, 387. [CrossRef]
32. EN 61140. *Protection against Electric Shock-Common Aspects for Installation and Equipment*; European Committee for Standards: Brussels, Belgium, May 2016.
33. Van Willigenburg, P.; Woudstra, J.; de Lange, T.; Stokman, H. First step to full DC-potential: Improving energy efficiency in household equipment. In Proceedings of the DUE 22nd Domestic Use of Energy, Cape Town, South Africa, 1–2 April 2014; pp. 1–7. [CrossRef]
34. Keleş, C.; Karabiber, A.; Akcin, M.; Kaygusuz, A.; Alagoz, B.B.; Gul, O. A smart building power management concept: Smart socket applications with DC distribution. *Int. J. Electr. Power Energy Syst.* **2015**, *64*, 679–688. [CrossRef]
35. Taufik, T. The DC House project: An alternate solution for rural electrification. In Proceedings of the IEEE Global Humanitarian Technology Conference (GHTC), San Jose, CA, USA, 10–13 October 2014; pp. 174–179. [CrossRef]
36. Malan, W.L.; Vilathgamuwa, D.M.; Walker, M.; Hiller, G.R. A three port resonant solid state transformer with minimized circulating reactive currents in the high frequency link. In Proceedings of the 2016 IEEE 2nd Annual Southern Power Electronics Conference (SPEC), Auckland, New Zealand, 5–8 December 2016; pp. 1–6. [CrossRef]
37. Papadimitriou, C.; Zountouridou, E.; Hatziargyriou, N. Review of hierarchical control in DC microgrids. *Electr. Power Syst. Res.* **2015**, *122*, 159–167. [CrossRef]
38. Bignucolo, F.; Raciti, A.; Caldon, R. Coordinating active and reactive energy balances in islanded networks supported by renewables and BESS. In Proceedings of the RPG 3rd Renewable Power Generation Conference, Naples, Italy, 24–25 September 2014; pp. 1–6. [CrossRef]
39. Rodrigues, W.A.; Santana, R.A.S.; Cota, A.P.L.; Oliveira, T.R.; Morais, L.M.F.; Cortizo, P.C. Integration of solid state transformer with DC microgrid system. In Proceedings of the 2016 IEEE 2nd Annual Southern Power Electronics Conference (SPEC), Auckland, New Zealand, 5–8 October 2016; pp. 1–6. [CrossRef]

40. Chen, Q.; Liu, N.; Hu, C.; Wang, L.; Zhang, J. Autonomous Energy Management Strategy for Solid-State Transformer to Integrate PV-Assisted EV Charging Station Participating in Ancillary Service. *IEEE Trans. Ind. Inform.* **2017**, *13*, 258–269. [CrossRef]
41. Blazic, B.; Papic, I. Voltage profile support in distribution networks-influence of the network R/X ratio. In Proceedings of the PEMC Power Electronics and Motion Control Conference, Poznan, Poland, 1–3 September 2008; pp. 2510–2515. [CrossRef]